The Mechanism of Denaturation and the Unfolded State of the α-Helical Membrane-Associated Protein Mistic

Tomas Jacso,[‡,†,§,⊥] Benjamin Bardiaux,[§,#] Jana Broecker,[∥] Sebastian Fiedler,[∥] Tom Baerwinkel,[‡,†] Andi Mainz,[‡,§] Uwe Fink,[§] Carolyn Vargas,[∥] Hartmut Oschkinat,[§] Sandro Keller,*,[∥] and Bernd Reif*,[‡,†,§]

[‡]Center for Integrated Protein Science Munich, Department Chemie, Technische Universität München, Lichtenbergstraße 4, 85747 Garching, Germany

[†]Helmholtz-Zentrum München, Deutsches Forschungszentrum für Gesundheit und Umwelt, Ingolstädter Landstraße 1, 85764 Neuherberg, Germany

[§]Leibniz-Institut für Molekulare Pharmakologie, Robert-Rössle-Straße 10, 13125 Berlin-Buch, Germany

[∥]Molecular Biophysics, University of Kaiserslautern, Erwin-Schrödinger-Straße 13, 67663 Kaiserslautern, Germany

S *Supporting Information*

ABSTRACT: *In vitro* protein-folding studies using chemical denaturants such as urea are indispensible in elucidating the forces and mechanisms determining the stability, structure, and dynamics of water-soluble proteins. By contrast, α-helical membrane-associated proteins largely evade such approaches because they are resilient to extensive unfolding. We have used optical and NMR spectroscopy to provide an atomistic-level dissection of the effects of urea on the structure and dynamics of the α-helical membrane-associated protein Mistic as well as its interactions with detergent and solvent molecules. In the presence of the zwitterionic detergent lauryl dimethylamine

oxide, increasing concentrations of urea result in a complex sequence of conformational changes that go beyond simple two-state unfolding. Exploiting this finding, we report the first high-resolution structural models of the urea denaturation process of an α-helical membrane-associated protein and its completely unfolded state, which contains almost no regular secondary structure but nevertheless retains a topology close to that of the folded state.
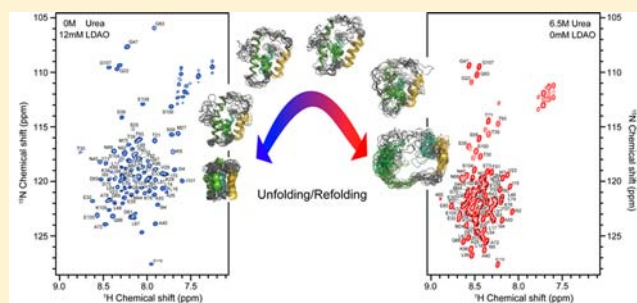
INTRODUCTION

The principles governing the folding of soluble[1] and β-barrel membrane proteins[2−4] are increasingly well understood. This is in great part due to *in vitro* experiments relying on the protein-destabilizing properties of chemical denaturants such as urea and guanidinium chloride.[5,6] A similarly detailed understanding of the folding of α-helical membrane proteins is highly desirable, not least because many of them are implicated in misfolding diseases.[7] However, progress in this field is lagging behind because of experimental and conceptual challenges resulting from the tight association of membrane proteins with lipid bilayer membranes or membrane-mimetic systems such as detergent micelles.[8] In particular, although urea and guanidinium chloride can affect solvent-exposed loop regions and disrupt helix−helix interactions, they are not effective in completely unfolding α-helical membrane proteins in the presence of membrane-mimetic environments.[9] The same is true even for harsh detergents;[10−13] furthermore, the denatured, membrane-bound state induced this way is only vaguely understood both structurally and thermodynamically,[14] making membrane proteins rather poor targets for chemical-unfolding assays.

For water-soluble proteins, group-transfer free energies[15] as well as hydrogen-exchange experiments[16] strongly imply that interactions between urea and the polypeptide backbone play a dominant role in driving the unfolding process. This view has recently been supported by NMR and small-angle X-ray scattering data[17] on the unfolded state of the model protein ubiquitin, demonstrating extensive interactions between urea and the polypeptide backbone. Molecular dynamics (MD) simulations on the same protein[18] suggest that the main contribution to the destabilization of the native fold comes from dispersion interactions with nonpolar side chains, in agreement with earlier MD simulations for lysozyme[19] and Trp-cage miniprotein.[20] Hence, while a consensus is emerging that the destabilizing effect of urea is primarily due to direct interactions with protein moieties that become exposed on unfolding, the exact nature of these interactions is still under debate. The situation is even more obscure for α-helical membrane proteins associated with membrane-mimetic environments. Specifically, it remains unclear whether the resistance of membrane proteins against chemical unfolding is a direct
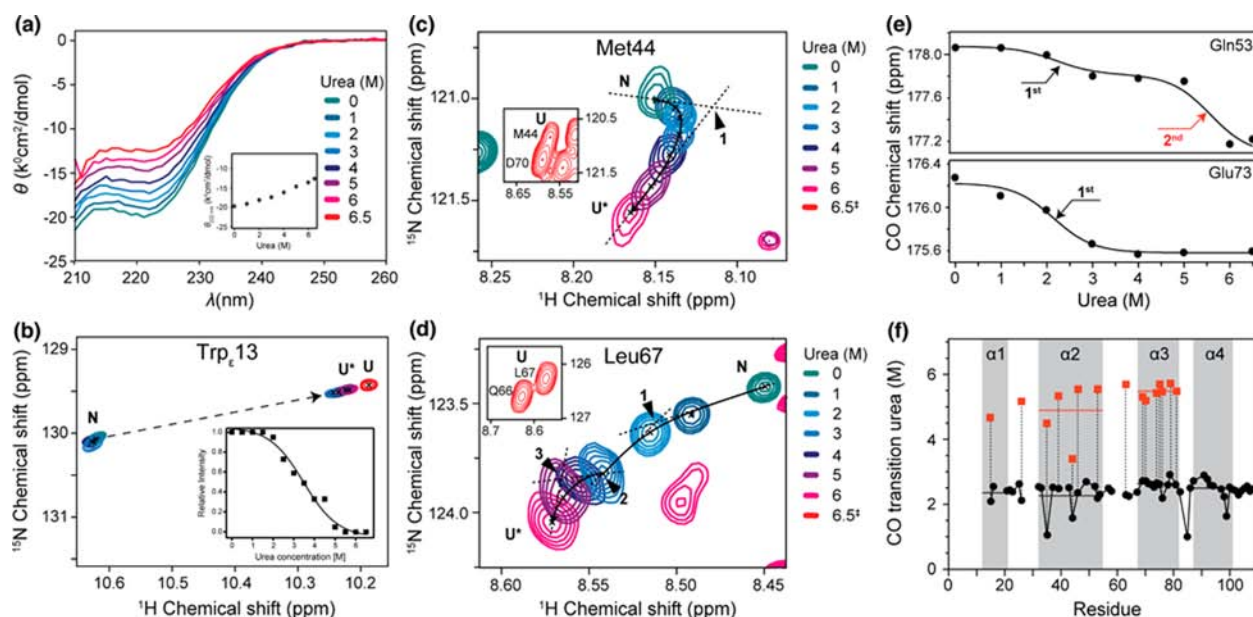
Figure 1. Urea-induced structural transitions of Mistic. (a) Circular dichroism spectra at 20 °C in 50 mM Tris-HCl, pH 7.4 in the presence of 12 mM LDAO and increasing urea concentrations. (b) ^{1}H,^{15}N correlation spectrum of the Trp-13 indole resonance. The inset shows the relative Trp$_\varepsilon$-13 HSQC cross peak intensities of the native state as a function of urea concentration, indicating a two-state transition. (c,d) Backbone resonances in the ^{1}H,^{15}N correlation spectrum reveal a more complicated behavior that cannot be fit assuming a two-state process. Correlation signals for Met-44 and Leu-67 are shown as examples. The native state at 0 M urea, the denatured state at 6.5 M urea in the presence of 12 mM LDAO, and the unfolded state at 6.5 M urea in the absence of detergent are denoted as N, U*, and U, respectively. (e) CO chemical shift changes upon titration with urea. Glu-73 and Gln-53 represent typical examples of residues that follow a two-state and a more complex process, respectively. (f) Midpoints of CO chemical shifts upon titration with urea plotted versus Mistic sequence. First and second transitions are labeled by black circles and red squares, respectively. Horizontal lines indicate average transition values of individual helical segments. NMR experiments were carried out at 37 °C in 50 mM Tris-HCl, pH 7.4 in the presence of 0−6.5 M urea.

consequence of their pronounced hydrophobicity or rather results from the solvent-shielding effect of the membrane-mimetic system used for solubilization.[8]

To address this question, we have set out to monitor the influence of urea on the structure and dynamics of the α-helical membrane-associated protein Mistic solubilized in detergent micelles composed of the zwitterionic detergent lauryl dimethylamine oxide (LDAO). For the present purpose, Mistic offers several advantages over more canonical membrane proteins: (i) Its four-helical bundle structure in the presence of LDAO has been solved by solution-state NMR spectroscopy,[21] thus enabling atomistic-resolution insights into its interactions with solvent, detergent, and denaturant.[22] (ii) For a membrane-associated protein, Mistic is rather small and contains an unusually large fraction of polar residues, which we speculated might render the unfolded polypeptide soluble at high urea concentrations. (iii) Nevertheless, Mistic displays many of the hallmarks of more hydrophobic α-helical membrane proteins, including tight association with membranes both *in vivo*[21] and *in vitro*,[23] aggregation and precipitation in the absence of membrane-mimetic systems,[21,24] and, upon solubilization in LDAO, direct interactions with detergent molecules arranged around the protein in two apposing layers.[21] (iv) Controversial claims regarding Mistic's folding core provide an interesting working hypothesis for protein-folding experiments. In particular, the conclusion from MD simulations[25] that the folding core resides in the N-terminus is hard to reconcile with the discovery of N-terminally truncated homologues lacking the first helical segment.[26] (v) Finally, a better understanding of Mistic's folding behavior may aid in exploiting its chaperoning activity for the recombinant

production, bilayer insertion, and detergent solubilization of other membrane proteins.[27,28] Thus, while Mistic differs in a number of aspects from larger and more hydrophobic, integral membrane proteins, it is a promising model for extending established approaches to the elucidation of the influence of urea on a protein associated with a membrane-mimetic environment.

■ RESULTS

LDAO-Solubilized Mistic Is Not a Two-State Folder. To shed light on the effect of a chemical denaturant on protein conformation and solvent interactions in a membrane-mimetic environment, Mistic solubilized in LDAO micelles was titrated with increasing concentrations of urea. Circular dichroism (CD) spectroscopy (Figure 1a) suggested an α-helix content of about 60% in the absence of urea, which is in very good accord with the NMR structure of folded Mistic.[21] Stepwise addition of urea resulted in a moderate decrease in CD signal intensity, but helical secondary structure remained pronounced at >40% even in the presence of 6.5 M urea. This is in agreement with chemical shift information from heteronuclear NMR experiments (Figure S1), which indicated that the major secondary-structure elements are maintained during the titration, thus paving the way for a detailed study of the denaturation process. While intrinsic tryptophan and tyrosine fluorescence experiments showed that the polarity of the solvent environment does not change considerably upon addition of urea (Figure S2a), solution-state NMR heteronuclear single-quantum correlation (HSQC) titration experiments revealed an apparent two-state transition of the Trp-13 indole resonance (Figure 1b). In the folded state,[21] the indole group of Trp-13 in helix 1
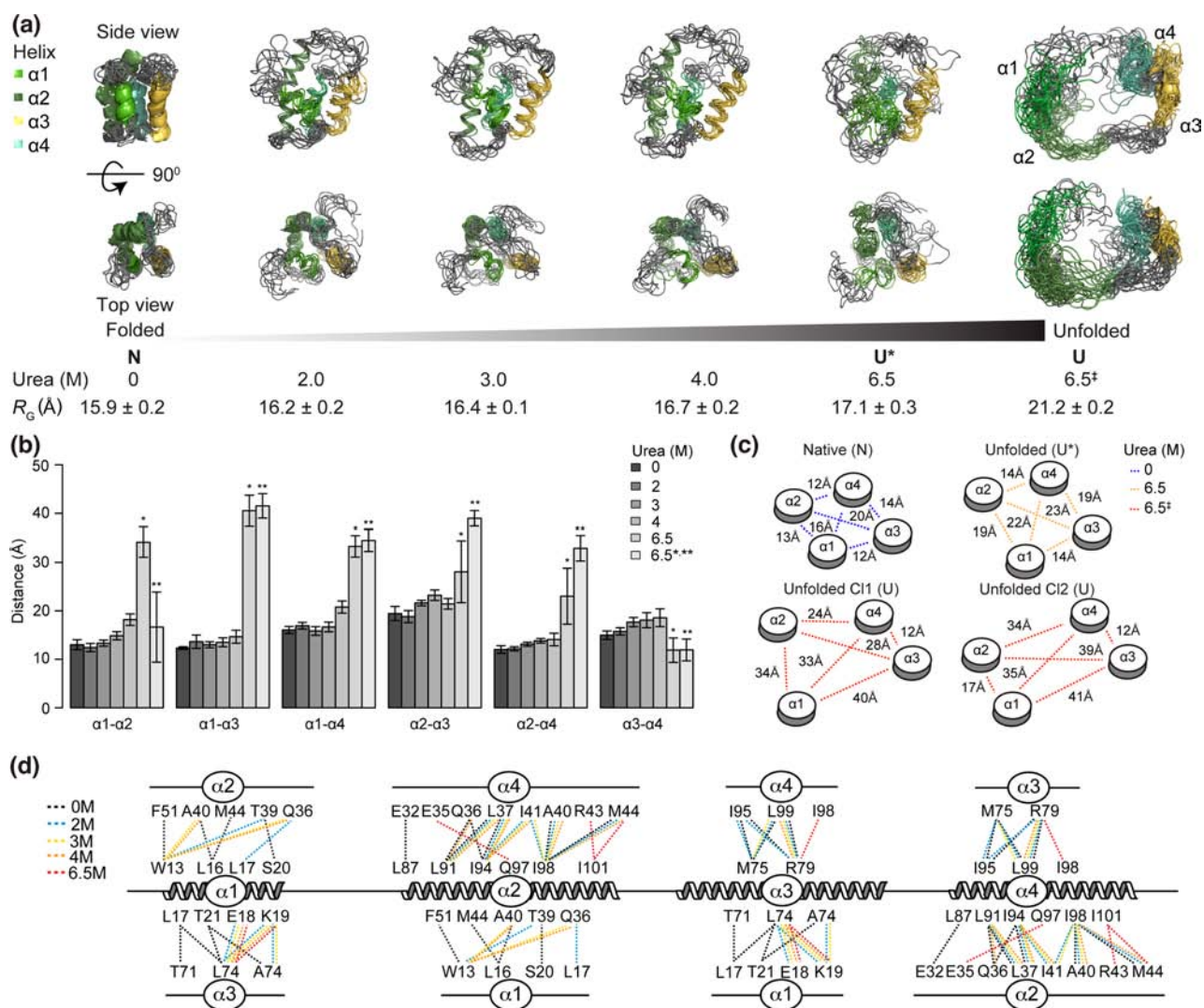
Figure 2. Structural characterization of the unfolding process of Mistic. (a) Structural ensembles as a function of urea concentration. The 10 lowest-energy structures in the structural ensembles are shown together with the radius of gyration calculated for each ensemble. The native state at 0 M urea, the denatured state at 6.5 M urea in the presence of 12 mM LDAO, and the unfolded state at 6.5 M urea in the absence of detergent are denoted as N, U*, and U, respectively. For each structural ensemble, the corresponding calculated radius of gyration (R_G) is given. (b) Helix−helix distances derived from the structural ensembles. The two main clusters, Cl1 and Cl2, of the unfolded state in the absence of LDAO are labeled * and **, respectively. (c) Schematic representation of helix−helix distances in the native (N) and denatured (U*) states in the presence of 12 mM LDAO and in the two major clusters Cl1 and Cl2 of the unfolded (U) state in the absence of LDAO. (d) Side-chain contacts in the structural ensembles of Mistic as a function of urea concentration.

is buried inside the protein and is involved in π-stacking interactions with the aromatic side chain of Phe-51 in helix 2. Upon addition of urea, this interaction is lost, resulting in a large chemical shift change indicating dissociation of helix 1 from the remaining bundle consisting of helices 2, 3, and 4. This interpretation is in agreement with the observation that the N-terminal helix is dispensable for both the structural integrity and the chaperoning ability of Mistic,[26] but it challenges MD simulations[25] suggesting that the folding core comprises an N-terminal helical bundle.

In contrast with this side-chain resonance, all backbone resonances in the HSQC spectra revealed a more intricate mechanism exceeding that of a simple two-state process (Figure 1c,d). Therefore, we extracted $C\alpha$, CO chemical shifts at several urea concentrations (Figure S1), because these are particularly susceptible to conformational changes and can serve as probes of secondary-structure formation and hydrogen bonding.[29] In

the presence of LDAO, $C\alpha$, CO chemical shifts indicated a high degree of α-helical structural propensity even under strongly denaturing conditions of 6.5 M urea. For most residues, the CO chemical shift apparently followed a two-state process with a transition midpoint around (2.5 ± 0.4) M urea. For a subset of residues, however, the urea dependence of the CO chemical shifts revealed a more complex pattern characterized by a second transition with a midpoint at 5.0 ± 1.0 M urea (Figure 1e,f). Interestingly, chemical shifts that reveal such three-state transitions are found for residues at positions $i,i+4$ in the sequence, hinting at helix−helix interactions that are lost only at rather high denaturant concentrations. Relaxation experiments in fact showed that helices 3 and 4 may still interact at a urea concentration of 6.5 M, whereas almost complete loss of α-helical secondary structure is observed only after removal of LDAO (see below).
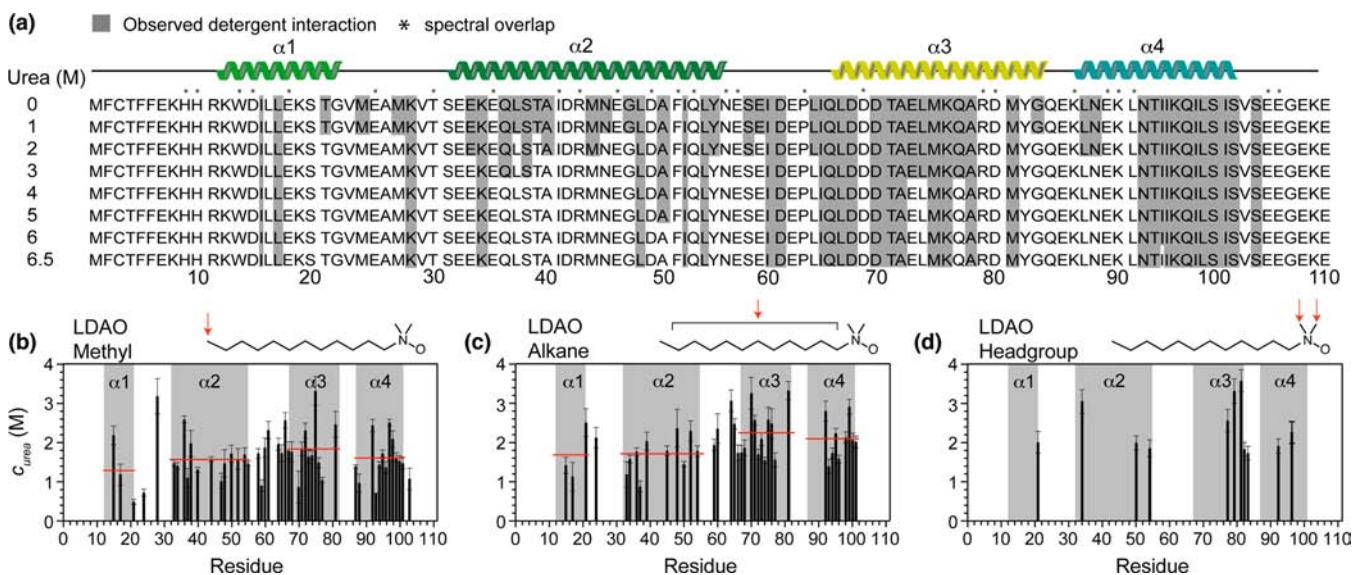
Figure 3. Changes in protein–detergent interactions upon urea titration. (a) NOEs between the backbone of Mistic and the alkyl chain of LDAO are indicated as gray boxes as a function of amino acid sequence. Residues that are not resolved because of spectral overlap are labeled *. (b–d) Site-specific protein–detergent affinities. c_{urea} refers to the urea concentration at which the protein–detergent NOE intensity is reduced to 50%, which is plotted separately for the terminal methyl group, the alkane moiety, and the headgroup of LDAO. Red lines indicate average c_{urea} values of individual helical segments. NMR experiments were carried out at 37 °C in 50 mM Tris-HCl, 12 mM LDAO, pH 7.4, and increasing concentrations of urea as indicated.

**Urea Causes Gradual Helix Fraying but Does Not Abolish Secondary Structure.** To identify structural changes of Mistic in the presence and absence of LDAO, we carried out paramagnetic relaxation enhancement (PRE) measurements.[30] To this end, spin labels were engineered into five positions (S3C, T30C, S58C, N88C, and E110C) to yield long-range distance information.[21] These PRE distance restraints (Figure S3) together with dihedral angle information from Cα, CO chemical shift data were used for structure calculations at 0–6.5 M urea in the presence of 12 mM LDAO and, additionally, at 6.5 M urea in the absence of detergent (Figure 2). The NMR data were supported by dynamic light scattering (DLS) experiments (Figure S2b) demonstrating that the diameter of the protein–detergent complex increases when the urea concentration is raised, in stark contrast with the urea-induced shrinking of protein-free detergent micelles.[31] Although the protein–detergent complex expands, the individual secondary-structure elements are maintained. However, the distribution of Φ, Ψ angles in the ensembles indicated sampling of a larger conformational space (Figure S4a), implying formation of noncanonical hydrogen bonds, in particular between residues $i,i+2$, $i,i+3$, and $i,i+5$. Statistical analysis of the structural ensemble showed that, at low urea concentrations, $i,i+3$ and $i,i+4$ hydrogen bonds dominate over the complete length of each helix. At higher urea concentrations, the helix termini become increasingly involved in $i,i+2$ hydrogen-bonding contacts, whereas the central regions of the helices retain $i,i+3$ and $i,i+4$ hydrogen bonds (Figure S4b), demonstrating that the primary effect of urea on protein structure consists in the fraying of individual helices. This is consistent with the finding that backbone hydrogen bond patterns shift during helix conformational changes in the functional cycle of bacteriorhodopsin.[32]

Interactions with Detergent Prevent Secondary-Structure Disruption. Protein–detergent interactions were observed by monitoring NOEs between amide groups of the polypeptide backbone and detergent protons (Figure 3). Among all observable residues, the fraction of residues exhibiting NOEs with LDAO moieties decreases from 50% to 28% as the urea concentration is increased from 0 to 6.5 M. Intriguingly, there is no obvious specificity with respect to the type of amino acid but rather a strong correlation between protein–detergent interactions and secondary structure. Transition midpoints extracted from the urea concentration dependence of the NOE intensities (Figure S5) revealed that helix 3 has overall the strongest affinity for LDAO, followed by helices 4, 2, and 1. These NOE transitions are in agreement with the first transition observed in CO chemical shift titration experiments (Figure 1f), again reflecting the coupling of secondary-structure formation with protein–detergent interactions. In the presence of LDAO, no correlations between the protein and urea were detected in NOESY-type experiments (Figure S6), implying that urea cannot access most of the polypeptide backbone of LDAO-solubilized Mistic, which is in stark contrast with the detergent-free unfolded state of water-soluble proteins such as ubiquitin.[17] In line with our observations, backbone burial in a micellar environment has recently been suggested to account for the marginal effects observed for some protein-stabilizing osmolytes on the stability of peripheral myelin protein 22 (PMP22).[13] Urea has been shown to render detergent micelles less compact, increasing headgroup solvation and alkyl chain dynamics.[31,33] Such loosening of the detergent assembly around the protein might explain urea-induced, partial unfolding of Mistic in the presence of LDAO and is, in fact, also reflected in the gradual increase in the hydrodynamic radius of the protein–detergent complex, while the radius of the protein itself remains almost unchanged (Figure S2).

Detergent Removal Results in an Unfolded Chain with Native-State Topology. In light of the above correlation between protein–detergent interactions and secondary structure, we sought to unfold Mistic to a greater extent by

removing the detergent in the presence of 6.5 M urea. Indeed, this resulted in virtually complete unfolding of the polypeptide chain, as only helix 3 retained helical propensity on the order of 30% in the absence of LDAO (Figure 4a). This is in agreement
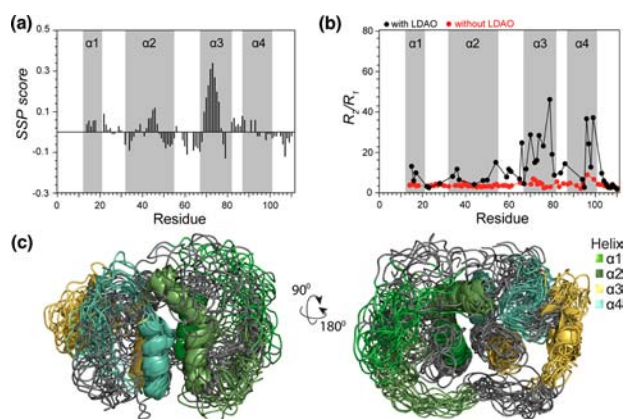
Figure 4. Characterization of the unfolded state of Mistic in the absence of detergent. (a) Secondary-structure propensity (SSP) at 6.5 M urea in the absence of detergent calculated using the program SSP.[35] Only helix 3 retains significant secondary-structure propensity on the order of 30%. (b) R_2/R_1 relaxation rates at 6.5 M urea in the absence (red) and presence (black) of 12 mM LDAO. The detergent stabilizes helices 3 and 4, resulting in slow local dynamics. (c) Superposition of the native and the completely unfolded (Cluster 1) structural ensembles. Although no secondary structure is observed in the unfolded state, the overall topology of the native state is retained. NMR experiments were carried out at 37 °C in 50 mM Tris-HCl, pH 7.4, 6.5 M urea either with or without 12 mM LDAO.

with secondary-structure prediction based on AGADIR,[34] which indicates helical propensity for helix 3 only. R_1 and R_2 relaxation experiments yielded information on the local dynamical properties at different urea concentrations (Figures 4b and S7). Under strongly denaturing conditions of 6.5 M urea in the absence of LDAO, we detected fast dynamics for all residues, underlining the virtually complete loss of secondary structure. By contrast, in the presence of LDAO, the dynamics of helices 3 and 4 is comparable to that in the native state, whereas the rest of the protein remains unstructured at high urea concentrations. Structure calculations employing PRE and chemical shift data as restraints yielded two major structural clusters, Cl1 and Cl2, of the detergent-free unfolded state (Figure S8). Superposition of the structural ensembles of the native state and the unfolded state (Cl1) in the absence of detergent (Figure 4c) revealed a remarkable similarity in topology between the two states. Though the unfolded state is more loosely packed and contains virtually no regular structure, the relative positioning of the secondary-structure elements in the native state is retained in the unfolded state.

Residual secondary structure,[36,37] long-range interactions,[38] and native-state topology[39,40] in the unfolded state have been reported for soluble globular proteins, where they might accelerate the folding process by productively biasing the transition from the unfolded-state ensemble to the unique fold of the native state.[41] Interactions with detergent and concomitant structural rearrangements under denaturing conditions have been observed for the β-barrel membrane protein OmpX[42] and even for the water-soluble protein 434-repressor(1−63).[36] In both cases, residual structure in the absence of detergent and detergent binding are restricted to

hydrophobic patches in the unfolded state.[42] The present data demonstrate, however, that hydrophobicity is not a stringent requirement, as most of the residues in helix 3 of Mistic are polar. Of special note in this context is the observation of strong, urea-resistant NOEs between the C-terminal end of helix 3 and the zwitterionic headgroup of LDAO (Figure 3d). Thus, while binding of detergent and induction of structure preferentially affect slightly prestructured regions also in Mistic, the driving forces are, at least in part, polar in nature, as has been observed for the interactions among designed trans-membrane helices embedded in a hydrophobic milieu.[43]

***In Vitro* Folding Experiments Rationalize Earlier Experimental Findings.** All urea-induced changes in the conformation of Mistic as well as its interactions with LDAO and solvent were found to be completely reversible at the microscopic level. Thus, renaturation from the urea-denatured state corresponded to the exact reversal of the sequence of events described above: removal of denaturant from detergent-solubilized Mistic resulted in successive formation of secondary structure, yielding first noncanonical and then increasingly canonical hydrogen bonds in the polypeptide backbone. Simultaneously, a growing number of protein−detergent NOEs were observed, indicating compaction of the protein. Hence, in the presence of LDAO, the assembly process starts from a folding core consisting of helices 3 and 4, which are present even at 6.5 M urea, and then proceeds through recruitment of helix 2 and finally helix 1, which is the least stable and is formed only under almost native conditions. This is in contrast with what has been concluded from MD simulations implying that the folding core resides in the N-terminal part of Mistic.[25] However, our observations are in agreement with the fact that helix 1 is dispensable for both the structural integrity and the chaperoning ability of Mistic.[26] Moreover, the low stability of helix 1 of LDAO-solubilized Mistic is reminiscent of the reduced stability of the first transmembrane helix of the trembler-J (TrJ) disease mutant L16P of PMP22, inducing enhanced dissociation from the other helices and, eventually, loss of function.[44]

The present data are also in accord with the finding that substitution of Met-75 by an alanine residue destabilizes the protein and leads to its partitioning between the membrane and the cytoplasm.[21] Met-75 is located in helix 3 and is involved in contacts with residues Ile-95 and Leu-99 in helix 4. Interactions among aliphatic side chains thus seem to be crucial for the structural integrity and stability of the folding core of Mistic (Figure 2d). Even though polar side chains are present at an unusually high density and seem to be involved in LDAO binding and ensuing secondary-structure induction under denaturing conditions, they play only a secondary role during the further assembly of the four-helix bundle. Rather, compaction under more native conditions is promoted primarily by hydrophobic side-chain interactions, which appear to be more favorable than protein−detergent interactions. This is most likely due to more efficient packing resulting from interdigitation of side chains at helix−helix interfaces[45] as compared with the perpendicular orientation of protein side chains with respect to detergent alkyl chains.

■ DISCUSSION

The results reported herein provide detailed insights into structural and dynamical changes occurring when the α-helical protein Mistic solubilized in LDAO micelles is exposed to increasing concentrations of urea. Chemical shifts and PRE

distance restraints yielded a detailed view of gradual changes in protein structure, while protein–detergent interactions were monitored using NOEs. Most approaches developed for *in vitro* studies of soluble-protein folding are not readily applicable to α-helical membrane proteins. The primary reason for this is the fact that chemical denaturants such as urea or guanidinium chloride are not capable of completely unfolding such proteins, although they do have a major impact on protein structure and dynamics within lipid membranes and membrane-mimetic systems.[8,9] In line with this, we found that, in the presence of LDAO micelles, urea cannot access most of the polypeptide backbone of Mistic, even though the latter is an unusually hydrophilic membrane-associated protein. Considerable parts of the protein remain shielded by detergent and thus are forced to retain secondary structure, because the disruption of backbone hydrogen bonds would be energetically too costly in the low-dielectric medium provided by the detergent environment.[46] In particular, helices 3 and 4 have the highest affinity for LDAO and hence are most stable against unfolding. Therefore, as long as the protein is suspended in LDAO, a large amount of secondary structure and a considerable number of tertiary contacts persist even under strongly denaturing conditions. However, we could show that Mistic can be unfolded virtually completely upon removal of detergent. In the absence of detergent, only helix 3 retains some residual structure, but the topology of the native state is still remnant.

A full trajectory of a restrained MD simulation, containing morphed structural models of Mistic obtained over the entire range of urea and detergent concentrations, is shown in Supporting Movie S1: In the presence of LDAO, only helices 3 and 4 remain rigid at 6.5 M urea, forming the core of the structure and a scaffold for the assembly of the remaining parts of the protein. The *i,i*+4 periodicity of the urea concentration dependence of the CO chemical shift curves suggests helix–helix interactions involving helices 2 and 3, which finally recruit helix 1. These interhelical interactions take place at urea concentrations below 3.3 M, as revealed by fluorescence and NMR titration experiments, and coincide with the loss of detergent–protein NOEs, which manifests itself as an inflection point in the urea concentration dependence of the CO chemical shifts. Thus, folding of the membrane-associated protein Mistic in LDAO occurs through the stepwise formation of canonical hydrogen bonds within the secondary-structure elements and progresses through coordination of α-helices 3 and 4 and subsequent packing of helices 2 and 1 against this scaffold.

CONCLUSION

Using optical and NMR spectroscopy, we have shown how urea affects the structure and dynamics of the α-helical membrane-associated protein Mistic. In addition, we have probed the interactions of Mistic with both detergent and denaturant to contribute to a better understanding of their complex interplay within a micellar environment. We thus could show that strong, partly polar interactions with LDAO protect the protein against complete urea-induced unfolding but that the latter is possible in the absence of detergent. Current efforts are directed at extending these studies to other detergents to systematically assess the contributions of polar and nonpolar interactions to the stability of Mistic in a micellar environment.

METHODS

Cloning and Protein Production. Mistic was cloned from *Bacillus subtilis* into the expression vector pET30 (Novagen). A QuikChange mutagenesis kit (Stratagene) was used for removal of the only wild-type cysteine residue at position 3 (C3S) and for production of single-cysteine mutants to accommodate spin labels for PRE measurements (T30C, S58C, N88C, and E110C). The resulting plasmid was transformed into the *Escherichia coli* expression strain BL21(DE3). Unlabeled, u-^{15}N-, and u-^{13}C,^{15}N-labeled Mistic variants were produced. Cells were grown in unlabeled Luria broth (LB) until OD$_{600 \text{ nm}}$ = 0.6. For unlabeled Mistic, induction by 0.5 mM isopropyl-β-D-1-thiogalactopyranoside (IPTG) and expression were carried out in LB. For u-^{15}N- and u-^{15}N/^{13}C-labeled protein, medium exchange was performed prior to induction, cells were harvested at 4000 *g* for 10 min and resuspended in M9 minimal medium containing ^{15}N-NH$_4$Cl/^{12}C-glucose or ^{15}N-NH$_4$Cl/^{13}C-glucose as the sole sources of nitrogen and carbon, respectively. Cells were allowed to adapt for 15 min before induction.

Protein Purification. Cells were harvested by centrifugation at 6000 *g* for 15 min and resuspended in 20 mM Tris-HCl, 50 mM NaCl at pH 7.4 together with protease inhibitors (Complete EDTA-free, Roche). Cell lysis was achieved via five rounds of French press in the presence of DNase (DNase1, 3000 u/g cell pellet, AppliChem), 3 mM LDAO (Sigma-Aldrich), and 4 M urea (AppliChem), followed by centrifugation at 10000 *g* for 45 min to remove cellular debris, possible inclusion bodies, and DNA. Supernatant was loaded on a Ni-affinity column (GE Healthcare). The His-tagged protein was eluted using a 200 mM imidazole solution. The protein elution fraction was dialyzed against 20 mM Tris, 50 mM NaCl, 6 mM LDAO at pH 7.4 and subsequently treated with enterokinase (Novagen) overnight at room temperature. The cleaved protein was loaded onto an ion-exchange column (GE Healthcare) and eluted with 250 mM NaCl. The concentrated protein solution was then desalted and rebuffered into 20 mM Tris-HCl, pH 7.4, 50 mM NaCl, 12 mM LDAO. All samples were checked for purity and mass by SDS-PAGE and ^{1}H NMR.

Determination of Critical Micellar Concentrations by Isothermal Titration Calorimetry. Critical micellar concentrations (CMCs) were determined with the aid of isothermal titration calorimetry (ITC) experiments on a VP-ITC (GE Healthcare).[33] Automated peak integration and data analysis were performed as described in detail elsewhere.[47] All NMR experiments were carried out at an LDAO concentration of 12 mM, which is above the CMC of LDAO in the presence of 6.5 M urea (5.4 mM).

Circular Dichroism Spectroscopy. Purified Mistic in 50 mM Tris-HCl, pH 7.4, 50 mM NaCl, 12 mM LDAO was diluted into buffer A (50 mM Tris-HCl, pH 7.4, 50 mM NaCl, 10 mM LDAO, 5 mM DTT) and buffer B (50 mM Tris-HCl, pH 7.4, 50 mM NaCl, 10 mM LDAO, 5 mM DTT, 6.8 M urea) to yield a final protein concentration of 10 μM. For Mistic solutions at final urea concentrations of 1, 2, 3, 4, 5, 6, and 6.5 M, buffers A and B containing 10 μM Mistic were mixed and incubated for 16 h at room temperature. Far-UV CD measurements were performed on a Chirascan-plus spectropolarimeter (Applied Photophysics) in a polarimetrically checked quartz glass cuvette (Hellma) with an optical path length of 1 mm and a volume of 350 μL. Experimental settings included a wavelength increment of 1 nm, a digital integration time of 1 s, and a bandwidth of 1 nm. Samples were allowed to equilibrate for 3 min in the thermostated sample holder. CD spectra in the range 210–260 nm were recorded in triplicate at 20 °C; note that high concentrations of denaturant preclude the acquisition of reliable CD data at lower wavelengths.[48] Owing to the small size and compactness of the protein–detergent complex (Figure S2), light scattering is not an issue in this wavelength range. At each urea concentration, the averaged spectrum of three repeats was corrected by subtracting the corresponding buffer spectrum without protein as well as the offset signal at 250–260 nm. CD spectra were normalized with respect to protein concentration, number of residues, and path length to yield the mean residue molar ellipticity (θ, given in kdeg·cm^2/dmol). For estimation of helical secondary-structure contents, normalized CD spectra were

decomposed into the reference spectra of Brahms and Brahms[49] by nonlinear least-squares fitting.[50]

Fluorescence Spectroscopy. Samples were prepared as described above for CD spectroscopy. Intrinsic protein fluorescence measurements were performed on a Chirascan-plus spectropolarimeter (Applied Photophysics) equipped with an emission monochromator and a photomultiplier detector perpendicular to the excitation light beam. A quartz glass cuvette (Hellma) with an optical path length of 10 mm was used. Experimental settings included a wavelength increment of 1 nm, a digital integration time of 1 s, an excitation bandwidth of 1 nm, and an emission bandwidth of 14 nm. Samples were allowed to equilibrate for 3 min in the thermostated sample holder. Emission spectra in the range 310−500 nm were recorded in triplicate at 20 °C with an excitation wavelength of 280 nm. For each urea concentration, the averaged spectrum of three repeats was corrected by subtracting the corresponding buffer spectrum without protein and the offset signal at 490−500 nm. To obtain the wavelength of maximal fluorescence emission intensity, λ_{max}, spectra were fit according to Ladokhin et al.[51] using nonlinear least-squares fitting.

Dynamic Light Scattering. DLS experiments were performed on a ZEN3500 Zetasizer NanoZS instrument (Malvern Instruments) equipped with a 532-nm, 50-mW laser. The instrument detects backscattering at an angle of 173°. Samples containing 0.5, 1.0, or 1.5 mM Mistic in 20 mM Tris-HCl, pH 7.4, 50 mM NaCl, 6.5 M urea in the absence of LDAO were prepared to determine the hydrodynamic diameter of unfolded Mistic. LDAO was removed prior to the measurements by four consecutive rounds of washing with BioBeads (Bio-Rad Laboratories). Complete LDAO removal was confirmed by ^{1}H NMR experiments. The hydrodynamic diameter was also determined in the presence of 12 mM LDAO for the urea concentration range 0−6.5 M. All samples were subjected to centrifugation (10 min at 14 000 rpm at 37 °C) to thermally equilibrate and remove possible large particles. Experiments were performed at 37 °C in quadruplets. Each measurement consisted of 100 runs with a duration of 5 s each, thereby accumulating scattering data for a total of 500 s. The hydrodynamic diameter, D_H, was calculated using the software DTS 5.03 (Malvern Instruments).

NMR Experiments and Analysis. All Mistic samples were measured at 37 °C in 20 mM Tris-HCl buffer, pH 7.4, 50 mM NaCl, 0.01% NaN$_3$, 3 mM DTT, and 5% D$_2$O as lock solvent using protein concentrations in the range 0.2−1.5 mM. Highest-purity-grade urea (AppliChem) was dissolved in water and deionized with Serdolit MB (Serva Electrophoresis) before addition of Tris-HCl and NaCl. Samples containing 0.5−6 M urea were prepared from mixtures of stock solutions of 0 and 6.5 M urea.

We confirmed earlier chemical shift assignments of Mistic in LDAO[21] using 3D HNCA-BEST, HNCOCA-BEST, HNCO-BEST, HNCACO-BEST, ^{15}N-edited ^{1}H,^{1}H-NOESY, ^{1}H−^{15}N HSQC, ^{1}H−^{15}N SOFAST-HMQC, and hNcaNH experiments.[52−56] ^{1}H, ^{15}N, ^{13}Cα, ^{13}CO chemical shifts were used as site-specific probes of Mistic secondary structure in the presence of urea. ^{1}H, ^{15}N chemical shift changes were monitored for the urea concentration range 0−6.5 M in titration steps of 0.5 M urea. ^{1}H, ^{15}N, ^{13}Cα, and ^{13}CO chemical shifts were extracted from 3D BEST-HNCA and BEST-HNCO experiments at urea concentrations of 0, 1, 2, 3, 4, 5, 6, and 6.5 M in the presence of 12 mM LDAO. The experimental values were subtracted from random-coil ^{13}Cα and ^{13}CO chemical shifts to yield secondary-structure propensities.[57] For Mistic in 6.5 M urea in the absence of LDAO, the software SPP[35] was used to calculate secondary-structure propensity.

3D ^{15}N-edited ^{1}H,^{1}H-NOESY spectra were recorded to probe protein−detergent interactions. NOESY correlations among protein amide protons and CH$_3$−, CH$_2$−, and headgroup (CH$_3$)$_2$ resonances in 12 mM LDAO were encoded into the ^{1}H,^{15}N-dimension of the ^{15}N-edited ^{1}H,^{1}H-NOESY experiment. All cross-peak volumes were corrected according to the tumbling correlation time, τ_c, of the individual sample, and plotted as a function of the primary sequence. Urea-concentration-dependent NOE intensity data were employed to yield residue-specific affinities of Mistic for LDAO. The transition midpoint was taken as the urea concentration at which the NOE intensity dropped to 50% of the original value in the absence of urea.

All spin-labeled samples were uniformly ^{15}N isotopically enriched. For spin labeling, the protein was buffer-exchanged into 6.5 M urea. Samples were subsequently washed four times using BioBeads (Bio-Rad Laboratories) to remove the detergent. Attachment of the spin label was achieved as described earlier[30] using (S)-(2,2,5,5-tetramethyl-2,5-dihydro-1H-pyrrol-3-yl)methyl methanesulfonothioate) (MTSL; Toronto Research Chemicals) in the presence of 6.5 M urea. MTSL-labeled samples were then rebuffered into two stock solutions containing 20 mM Tris-HCl, pH 7.4, 50 mM NaCl, 12 mM LDAO, and either 0 or 6.5 M urea. In addition, MTSL-labeled Mistic samples were prepared in 6.5 M urea buffer without LDAO. PRE measurements of all MTSL-containing constructs were performed in the presence of 0−6.5 M urea and 12 mM LDAO as well as at 6.5 M urea in the absence of LDAO. Experiments were acquired and analyzed following the experimental procedures described by Battiste and Wagner.[30] ^{15}N R_1 and R_2 relaxation rates were determined as described earlier.[53]

■ ASSOCIATED CONTENT

ⓈSupporting Information

Detailed protocols for structural calculations as well as statistical analysis of Φ, Ψ-angles and hydrogen bonds; tables showing statistics of calculated structures and chemical shifts determined for Mistic at 0−6.5 M urea in the presence of 12 mM LDAO and at 6.5 M urea in the absence of LDAO; movie showing the unfolding and folding trajectories of Mistic as obtained from calculating 100 stepwise structural ensembles between experimentally determined structural ensembles. This material is available free of charge via the Internet at http://pubs.acs.org.

■ AUTHOR INFORMATION

Corresponding Authors
mail@sandrokeller.com
reif@tum.de

Present Addresses
⊥T.J.: AstraZeneca R&D Mölndal, Discovery Sciences, Pepparedsleden 1, SE-431 83 Mölndal, Sweden
#B.B.: Institut Pasteur, Unité de Bioinformatique Structurale, 25−28 rue du Dr Roux, 75724 Paris Cedex 15, France

Notes
The authors declare no competing financial interest.

■ REFERENCES

(1) Fersht, A. R. Nature Rev. Mol. Cell. Biol. 2008, 9, 650−654.
(2) Hong, H.; Tamm, L. K. Proc. Natl. Acad. Sci. U.S.A. 2004, 101, 4065−4070.
(3) Huysmans, G. H. M.; Baldwin, S. A.; Brockwell, D. J.; Radford, S. E. Proc. Natl. Acad. Sci. U.S.A. 2010, 107, 4099−4104.

(4) Moon, C. P.; Fleming, K. G. *Proc. Natl. Acad. Sci. U.S.A.* **2011**, *108*, 10174−10177.

(5) England, J. L.; Haran, G. *Annu. Rev. Phys. Chem.* **2011**, *62*, 257−277.

(6) Schellman, J. A. *Q. Rev. Biophys.* **2005**, *38*, 351−361.

(7) Sanders, C. R.; Myers, J. K. *Annu. Rev. Biophys. Biochem. Struct.* **2004**, *33*, 25−51.

(8) Fiedler, S.; Broecker, J.; Keller, S. *Cell. Mol. Life Sci.* **2010**, *67*, 1779−1798.

(9) Stanley, A. M.; Fleming, K. G. *Arch. Biochem. Biophys.* **2008**, *469*, 46−66.

(10) Lau, F. W.; Bowie, J. U. *Biochemistry* **1997**, *36*, 5884−5892.

(11) Otzen, D. E. *J. Mol. Biol.* **2003**, *330*, 641−649.

(12) Curnow, P.; Di Bartolo, N. D.; Moreton, K. M.; Ajoje, O. O.; Saggese, N. P.; Booth, P. J. *Proc. Natl. Acad. Sci. U.S.A.* **2011**, *108*, 14133−14138.

(13) Schlebach, J. P.; Peng, D.; Kroncke, B. M.; Mittendorf, K. F.; Narayan, M.; Carter, B. D.; Sanders, C. R. *Biochemistry* **2013**, *52*, 3229−3241.

(14) Renthal, R. *Biochemistry* **2006**, *45*, 14559−14566.

(15) Auton, M.; Holthauzen, L. M.; Bolen, D. W. *Proc. Natl. Acad. Sci. U.S.A.* **2007**, *104*, 15317−15322.

(16) Lim, W. K.; Rösgen, J.; Englander, S. W. *Proc. Natl. Acad. Sci. U.S.A.* **2009**, *106*, 2595−2600.

(17) Huang, J. R.; Gabel, F.; Jensen, M. R.; Grzesiek, S.; Blackledge, M. *J. Am. Chem. Soc.* **2012**, *134*, 4429−4436.

(18) Candotti, M.; Esteban-Martin, S.; Salvatella, X.; Orozco, M. *Proc. Natl. Acad. Sci. U.S.A.* **2013**, *110*, 5933−5938.

(19) Hua, L.; Zhou, R.; Thirumalai, D.; Berne, B. J. *Proc. Natl. Acad. Sci. U.S.A.* **2008**, *105*, 16928−16933.

(20) Canchi, D. R.; García, A. E. *Biophys. J.* **2011**, *100*, 1526−1533.

(21) Roosild, T. P.; Greenwald, J.; Vega, M.; Castronovo, S.; Riek, R.; Choe, S. *Science* **2005**, *307*, 1317−1321.

(22) Canlas, C. G.; Cui, T.; Li, L.; Xu, Y.; Tang, P. *J. Phys. Chem. B* **2008**, *112*, 14312−14318.

(23) Jacso, T.; Franks, W. T.; Rose, H.; Fink, U.; Broecker, J.; Keller, S.; Oschkinat, H.; Reif, B. *Angew. Chem., Int. Ed.* **2012**, *51*, 432−435.

(24) Debnath, D. K.; Basaiawmoit, R. V.; Nielsen, K. L.; Otzen, D. E. *Protein Eng. Des. Sel.* **2011**, *24*, 89−97.

(25) Psachoulia, E.; Bond, P. J.; Sansom, M. S. P. *Biochemistry* **2006**, *45*, 9053−9058.

(26) Roosild, T. P.; Vega, M.; Castronovo, S.; Choe, S. *BMC Struct. Biol.* **2006**, *6*, No. 10.

(27) Dvir, H.; Choe, S. *Protein Express. Purif.* **2009**, *68*, 28−33.

(28) Petrovskaya, L. E.; Shulga, A. A.; Bocharova, O. V.; Ermolyuk, Y. S.; Kryukova, E. A.; Chupin, V. V.; Blommers, M. J. J.; Arseniev, A. S.; Kirpichnikov, M. P. *Biochemistry—Moscow* **2010**, *75*, 881−891.

(29) Wang, Y.; Jardetzky, O. *Protein Sci.* **2002**, *11*, 852−861.

(30) Battiste, J. L.; Wagner, G. *Biochemistry* **2000**, *39*, 5355−5365.

(31) Patel, H.; Raval, G.; Nazari, M.; Heerklotz, H. *Biophys. Chem.* **2010**, *150*, 119−128.

(32) Cao, Z.; Bowie, J. U. *Proc. Natl. Acad. Sci. U.S.A.* **2012**, *109*, 8121−8126.

(33) Broecker, J.; Keller, S. *Langmuir* **2013**, *29*, 8502−8510.

(34) Muñoz, V.; Serrano, L. *Nat. Struct. Biol.* **1994**, *1*, 399−409.

(35) Marsh, J. A.; Singh, V. K.; Jia, Z.; Forman-Kay, J. D. *Protein Sci.* **2006**, *15*, 2795−2804.

(36) Neri, D.; Billeter, M.; Wider, G.; Wüthrich, K. *Science* **1992**, *257*, 1559−1563.

(37) Schwarzinger, S.; Wright, P. E.; Dyson, H. J. *Biochemistry* **2002**, *41*, 12681−12686.

(38) Klein-Seetharaman, J.; Oikawa, M.; Grimshaw, S. B.; Wirmer, J.; Duchardt, E.; Ueda, T.; Imoto, T.; Smith, L. J.; Dobson, C. M.; Schwalbe, H. *Science* **2002**, *295*, 1719−1722.

(39) Shortle, D.; Ackerman, M. S. *Science* **2001**, *293*, 487−489.

(40) Shortle, D. *Adv. Protein Chem.* **2002**, *62*, 1−23.

(41) Rose, G. D.; Fleming, P. J.; Banavar, J. R.; Maritan, A. *Proc. Natl. Acad. Sci. U.S.A.* **2006**, *103*, 16623−16633.

(42) Hiller, S.; Wider, G.; Imbach, L. L.; Wuthrich, K. *Angew. Chem., Int. Ed.* **2008**, *47*, 977−981.

(43) Tatko, C. D.; Nanda, V.; Lear, J. D.; DeGrado, W. F. *J. Am. Chem. Soc.* **2006**, *128*, 4170−4171.

(44) Sakakura, M.; Hadziselimovic, A.; Wang, Z.; Schey, K. L.; Sanders, C. R. *Structure* **2011**, *19*, 1160−1169.

(45) Eilers, M.; Shekar, S. C.; Shieh, T.; Smith, S. O.; Fleming, P. J. *Proc. Natl. Acad. Sci. U.S.A.* **2000**, *97*, 5796−5801.

(46) White, S. H.; von Heijne, G. *Curr. Opin. Struct. Biol.* **2005**, *15*, 378−386.

(47) Keller, S.; Vargas, C.; Zhao, H.; Piszczek, G.; Brautigam, C. A.; Schuck, P. *Anal. Chem.* **2012**, *84*, 5066−5073.

(48) Fiedler, S.; Cole, L.; Keller, S. *Anal. Chem.* **2013**, *85*, 1868−1872.

(49) Brahms, S.; Brahms, J. *J. Mol. Biol.* **1980**, *138*, 149−178.

(50) Kemmer, G.; Keller, S. *Nat. Protoc.* **2010**, *5*, 267−281.

(51) Ladokhin, A. S.; Jayasinghe, S.; White, S. H. *Anal. Biochem.* **2000**, *285*, 235−245.

(52) Lescop, E.; Schanda, P.; Brutscher, B. *J. Magn. Reson.* **2007**, *187*, 163−169.

(53) Cavanagh, J.; Fairbrother, W. J.; Palmer, A. G.; Skelton, N. J. *Protein NMR Spectroscopy: Principles and Practice*; Academic Press: San Diego, 1996.

(54) Schanda, P.; Kupce, E.; Brutscher, B. *J. Biomol. NMR* **2005**, *33*, 199−211.

(55) Weisemann, R.; Ruterjans, H.; Bermel, W. *J. Biomol. NMR* **1993**, *3*, 113−120.

(56) Panchal, S. C.; Bhavesh, N. S.; Hosur, R. V. *J. Biomol. NMR* **2001**, *20*, 135−147.

(57) Ulrich, E. L.; Akutsu, H.; Doreleijers, J. F.; Harano, Y.; Ioannidis, Y. E.; Lin, J.; Livny, M.; Mading, S.; Maziuk, D.; Miller, Z.; Nakatani, E.; Schulte, C. F.; Tolmie, D. E.; Wenger, R. K.; Yao, H.; Markley, J. L. *Nucleic Acids Res.* **2008**, *36*, D402−D408.

18891

dx.doi.org/10.1021/ja408644f | *J. Am. Chem. Soc.* 2013, 135, 18884−18891